

# Accurate new scaling routines for any table/function based FET model including temperature and noise behaviour

R. Follmann, R. Tempel, J. Herrmann, T. Sporkmann and I. Wolff, Fellow, IEEE

Institute of Mobile and Satellite Communication Techniques (IMST)  
Carl-Friedrich-Gauss-Straße 2, D-47475 Kamp-Lintfort, FRG  
phone #49 (2842) 981.226 Fax #49 (2842) 981.299 email: follmann@imst.de

## ABSTRACT

In this paper we present new scaling routines for any table/function based nonlinear FET model. These measurement based routines are very accurate and can also be used to calculate temperature behaviour. Also the prediction of noise behaviour is possible for scaled devices.

## INTRODUCTION

In the last few years many papers have been published concentrating either on noise or on temperature simulation [1] or on scaling routines for special effects like dispersion of the trans- and output conductance of a FET [2]. Our TOPAS (TransistOr PArAmeter Scaleable) called model is based on an accurate 2D spline table based model [3,4], which combines all the above counted effects within one model. The model has been expanded using two dimensional mathematical functions for describing the intrinsic nonlinear elements. Usually, simple scaling instructions (multiplication or division by 2) are used for scaling a device with the number of gatefingers  $N$  or the gatefinger width  $W_t$ . Our model uses new and accurate, measurement based scaling routines for all equivalent circuit elements. Furthermore, the same scaling functions can be used for describing the temperature behaviour of the model. The functions are also compatible with the noise simulation and can easily be implemented within every other nonlinear model. To our knowledge this is the first publication on overall scaleable table based models.

## EXTRINSIC SCALING PROCEDURE

The fact, that elements of a FET equivalent circuit scale with a factor of 2 (respectively 1/2) can not always be found, as shown in Figure 1 and Figure 2 for different extracted 0.25  $\mu\text{m}$  HEMT devices of the same technology. Some resistances are shown as  $1/R$  to get a scaling function proportional to  $N$  and  $W_t$ .

While the extrinsic resistances scale by a factor of approx. 1/2, the inductances except  $L_S$  remain nearly constant. In our model, which has been implemented into HP-EEsofs series IV (libra), the scaling of the extrinsic elements was taken into account by using a linear expression for  $S(N)$  as well as for  $S(W)$ , e.g.:

$$S_E(N) = a_{EN} \cdot N + b_{EN} \quad (1)$$

The constant coefficients  $a$  and  $b$  can be found by calculating a linear regression [5]. The whole extrinsic scaling function  $S_E$  is described as:

$$S_E(N, W) = S_E(N) \cdot S_E(W) \quad (2)$$

This function delivers even intermediate values useable e.g. for optimization purpose.

## INTRINSIC SCALING PROCEDURE

One main requirement for scaling the FETs intrinsic elements is the fact, that the intrinsic elements grids do not change their shapes when changing the device size (Figure 3 and Figure 4). Just the absolute values may change so that one element grid can be calculated from another by multiplying the first grid with a constant number  $c$ :

$$c = \frac{\sum_{V_{gs}, V_{ds}} \frac{G_x(V_{gs}, V_{ds})}{G_{ref}(V_{gs}, V_{ds})}}{n_{V_{gs}, V_{ds}}}, \quad (3)$$

whereby  $G_{ref}$  is a reference grid (the reference scaling factor is 1),  $G_x$  the scaled element grid and  $n$  the number of bias points taken into account. If the grids  $G_{ref}$  and  $G_x$  have been extracted for different bias points, they must be spline-interpolated to get the same reference of bias points. The second grid (Figure 4) can be calculated from the first grid (fig. 3) by a multiplication with  $c = 2.89$ . This value differs just a little from the usually calculated one

$$c_{old} = \frac{8 \times 75 \mu m}{4 \times 50 \mu m} = 3 \quad (4)$$

but is more accurate concerning the real device. All scaling values of the intrinsic elements for the examined HEMT devices can be seen in fig. 5 and 6. Most elements show an expected scaling behaviour except  $R_i$ , which is due to the fact, that  $R_i$  is one of the most frequency dependent elements and small variations of  $R_G$  and  $R_S$  may cause large variations of  $R_i$  during extraction process. Due to the constant grid shape the intrinsic scaling function  $S_I(N, W)$  can be calculated by superimposing both single scalings:

$$S_I(N, W) = S_I(N) \cdot S_I(W). \quad (5)$$

A test with the above mentioned  $c$  for scaling  $C_{gs}$  results in

$$\begin{aligned} c_{new} &= S_I(N = 4 \rightarrow N = 8) \\ &\cdot S_I(W = 50 \rightarrow W = 75) \\ &= 1.93 \cdot 1.49 = 2.88 \end{aligned} \quad (6)$$

In our model again a linear expression is used to get the intrinsic elements scaling functions, e. g.

$$S_I(W) = a_{IW} \cdot W + b_{IW}. \quad (7)$$

It must be pointed out, that a scaling value of 2.88 only means an error of 4% concerning a value of 3.0. But in worst case all scaling errors may sum up, so that one gets a much larger overall scaling error when using simple scaling factors.

## TEMPERATURE DEPENDENCE

For temperature calculations the same proposed scaling functions can be used. Now not different device sizes are scaled but  $I_{ds}(V_{gs}, V_{ds})$  of the same device at different temperatures. The maximum error that occurs, when scaling e. g. a  $I_{ds}$  grid from the reference temperature  $T = 293$  K to  $T = 253$  K using eq. 3, is less than 5% in the ohmic region and less than 1% in the saturation region. All scaling factors for scaling  $1/I_{ds}$  with temperature can be seen as dots in Figure 7.

The temperature behaviour including saturation effects (Figure 7) is modeled using eq. 8. Temperature dependence of the intrinsic  $R_i$  is been taken care of using eq. 9. As some measurements have shown, the temperature dependence of the capacitances can be neglected.

$$S_{1/I_{ds}}(T) = \begin{cases} a_{1T} \cdot T + b_{1T} & \text{for } T < T_2 \\ a_{2T} \cdot T + b_{2T} & \text{for } T_1 \leq T < T_2 \\ a_{3T} \cdot T + b_{3T} & \text{for } T \geq T_2 \end{cases} \quad (8)$$

$$R_i(T) = R_i(T_0) \cdot [\gamma_{R_i}(T - T_0) + 1] \quad (9)$$



## NOISE CALCULATIONS

For noise calculation adapted [6] noise equations are used. For a conductance of a noise resistance equation (10)

$$g_R = \frac{\langle i_{th}^2 \rangle}{4kT_0 \Delta f} \cdot \frac{T_{sim}}{T_0} \quad (10)$$

is used. The channel noise is modeled using equation (11)

$$g_{ids} = \left( \frac{1}{4kT_0} k_f \frac{I_{ds}^{a_f}}{f^b} + \frac{2}{3} \frac{T_0}{T_{sim}} \frac{\partial I_{ds}}{\partial V_{gs}} \right) \cdot \frac{T_{sim}}{T_0} \quad (11)$$

$T_{sim}$  is the temperature, for which the noise parameter should be calculated.  $T_0$  is the actual temperature,  $k_f$  and  $a_f$  are noise coefficients and  $b$  is the frequency exponent.

## COMPARISON OF THE SCALED MODEL

In this section verification for the scaled model in comparison with small signal S-parameter, noise and temperature measurements on unscaled devices is done to demonstrate the new scaling facilities of our model. Furthermore, an oscillator [7] is simulated temperature dependent.

The results of scaling a 4x50  $\mu\text{m}$  reference device up to a 8x75  $\mu\text{m}$  HEMT are shown in Figure 8 for a bias point of  $V_{gs} = 0$  V and  $V_{ds} = 2$  V. All other comparisons (up- and down-scaled) show the same excellent results for a huge range of bias points. In fig. 9 the measured  $s_{21}$  of a 4x40  $\mu\text{m}$  HEMT at  $T = 373$  K is compared with the simulated

one, scaled again from the reference device at  $T = 279$  K. Although for the scaled model only the gatefinger width is reduced by 20%, it can be seen, that our scaling functions are much more accurate than the simple scaling procedure. Fig. 10 shows the minimum noise figure  $NF_{min}$  simulated with the same model, but scaled down to a 40  $\mu\text{m}$  device.

All simulations show perfect agreement with measurements.

Figure 11 shows the frequency and the power of the output signal of an oscillator [7] in an interesting temperature range of  $-40$  °C to  $80$  °C. The frequency varies about 43 MHz and the output power about 0.6 dB. This figure shows, that even circuits containing 8 FET devices [7] can be simulated using the proposed scaling functions without any problems. The simulation has been performed using the TOPAS model [3] and HP-EEsofs series IV (libra).

## SUMMARY

We presented a FET model, that uses very accurate scaling routines. Furthermore, the same scaling routines are suitable for temperature calculations. Simulations using scaled models show perfect agreement with small signal S-parameter measurement for different temperatures and with noise measurements. The scaling functions have been added to our TOPAS [3] model within HP-EEsofs circuit simulation software series IV (libra).

## REFERENCES

- [1] F. Sinnesbichler, and T. Felgentreff, „Large Signal and Noise Modeling of HEMT devices including Frequency and Temperature Effects,“ Proc. of the 27<sup>th</sup> EuMC, Israel, pp.428-431, 1997
- [2] V. I. Cojoracu, and T. J. Brazil, „Scalability of DC/AC non-linear dispersion models for microwave FETs,“ IEEE-MTT-S International Microwave Symposium Digest, Denver 1997.
- [3] R. Follmann, R. Tempel, T. Sporkmann, and I. Wolff, „A new spline based FET model for MESFETs and HEMTs,“ Proc. of the 27<sup>th</sup> EuMC, Israel, pp. 1360-1366, 1997.
- [4] R. Follmann, W. Lütke, R. Tempel, and I. Wolff, „A new method for large signal FET modeling for use in MMIC frequency multipliers,“ IEEE Workshop on "Experimentally Based FET Device Modelling & Related Nonlinear Circuit Design", Kassel, pp. 24.1-24.4, 1997.



- [5] I.N. Bronstein, and K. Semendjajew, *Taschenbuch der Mathematik*, Verlag Harri Deutsch, Zürich and Frankfurt am Main, 1980.
- [6] P. Antognetti and G. Massobrio. *Semiconductor Device Modeling with SPICE*, McGraw-Hill, 1988
- [7] R. Tempel, W. Lütke, J. Herrmann, and I. Wolff, "Coplanar MMICs for Sensor Applications at 25 GHz," IEEE Intern. Theory and Techn. Symposium (MTT-S), pp. 277-280, June 17-21, San Francisco, USA, 1996.

**FIGURES**

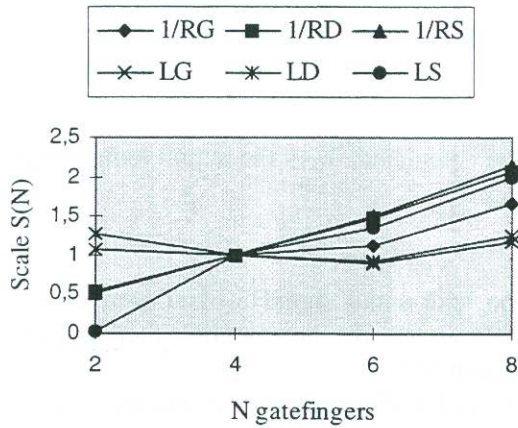


Figure 1: Scaling of extrinsic elements with number N of gatefingers, gatefinger width  $W_t=40\mu\text{m}$ .

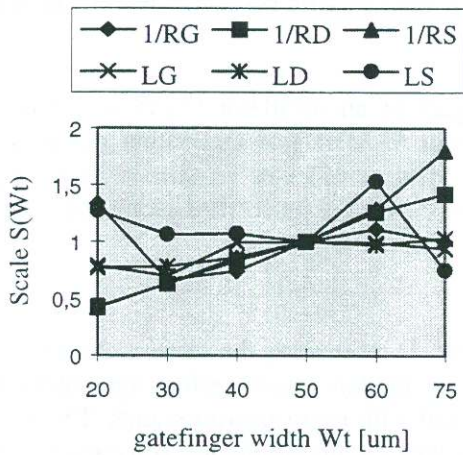


Figure 2: Scaling of extrinsic elements with gatefinger width  $W_t$ , number N of gatefingers  $N=4$ .

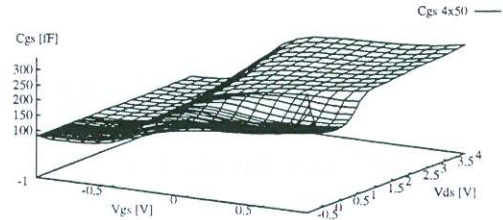


Figure 3: Intrinsic gate-source capacitance for the  $4 \times 50 \mu\text{m}$  HEMT.

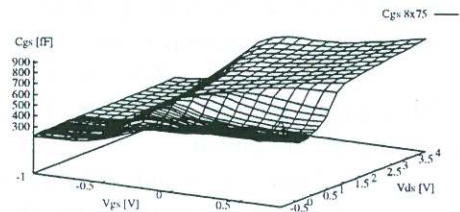


Figure 4: Intrinsic gate-source capacitance for the  $8 \times 75 \mu\text{m}$  HEMT.

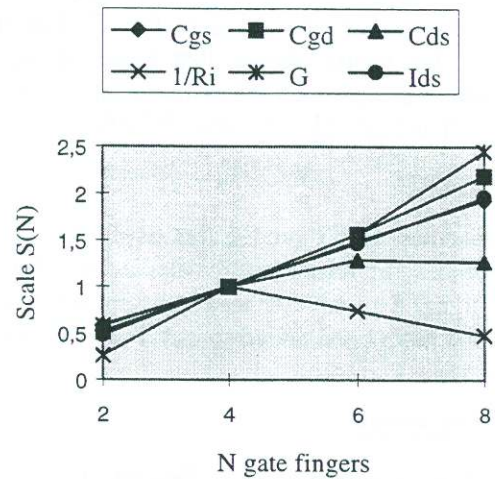


Figure 5: Scaling of intrinsic elements with number of gate fingers N.

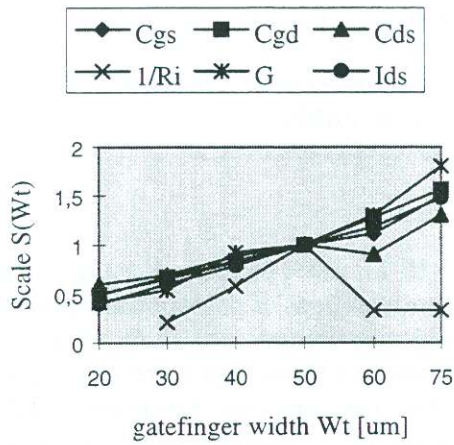


Figure 6: Scaling of intrinsic elements with gatefingewidth  $W_t$ .

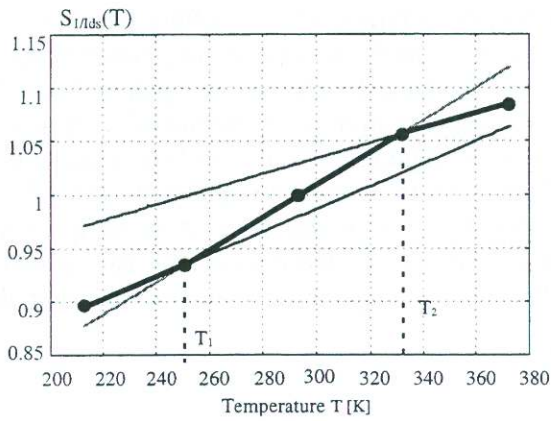


Figure 7: Scaling coefficients and straight lines.

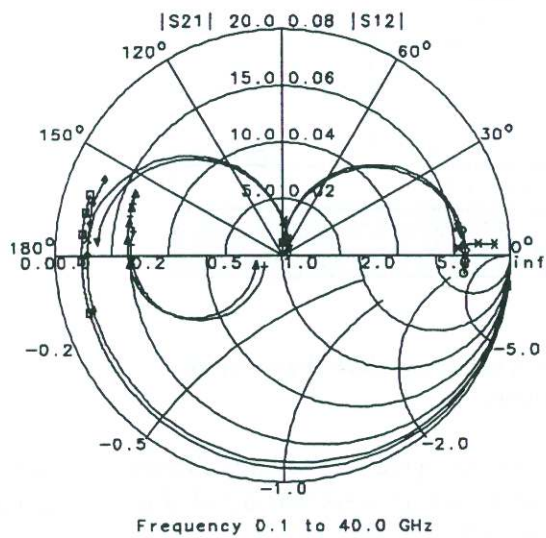


Figure 8: A  $4 \times 50 \mu\text{m}$  HEMT scaled to a  $8 \times 75 \mu\text{m}$  HEMT at  $V_{gs}=0\text{V}$  and  $V_{ds}=2\text{V}$ .

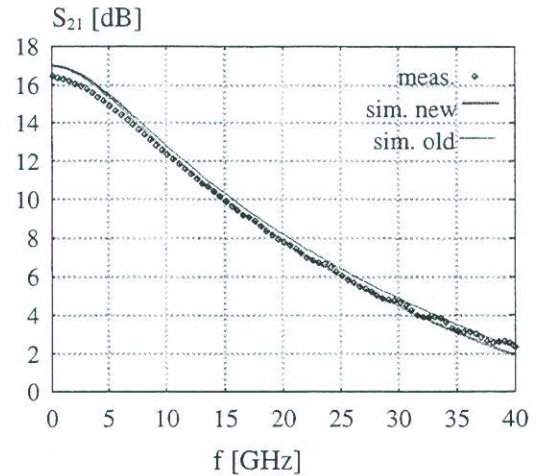


Figure 9: Simulation (simple and new scaling) vs. measurement of  $S_{21}$  of a  $4 \times 40 \mu\text{m}$  HEMT at  $T=373\text{K}$ . Model has been scaled from a  $4 \times 50 \mu\text{m}$  HEMT at  $T=293\text{K}$ . Bias point:  $0\text{V} / 2\text{V}$ .

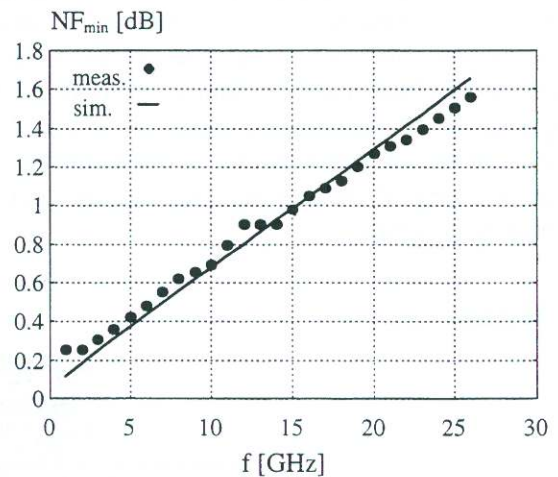


Figure 10: Simulation vs. measurement of  $NF_{\min}$  of a  $4 \times 40 \mu\text{m}$  HEMT at  $-0.1\text{V} / 2\text{V}$ . Model has been scaled from a  $4 \times 50 \mu\text{m}$  device.

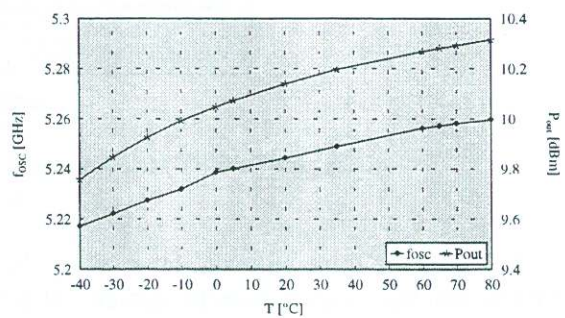


Figure 11: Simulation of oscillator frequency and output power vs. temperature.